Title: Refractory for Black Liquor Gasifiers

Type of Report: Quarterly Report

Reporting Period Start Date: October 1, 2004

Reporting Period End Date: December 31, 2004

Principal Authors: William L. Headrick Jr., Musa Karakus, Xiaoting Liang and Jun Wei

Date Report Issued: January 2005

DOE Award Number: DE-FC26-02NT41491

Name and Address of Submitting Organization:

Curators of the University of Missouri on behalf of University of Missouri-Rolla

Sponsored Programs

1870 Miner Circle

215 ME Annex

Rolla, MO 65409-1330

DISCLAIMER

This report was prepared as an account of work sponsored by an agency of the United States Government. Neither the United States Government nor any agency thereof, nor any of their employees, makes any warranty, express or implied, or assumes any legal liability or responsibility for the accuracy, completeness, or usefulness of any information, apparatus, product, or process disclosed, or represents that its use would not infringe privately owned rights. Reference herein to any specific commercial product, process, or service by trade name, trademark, manufacturer, or otherwise does not necessarily constitute or imply its endorsement, recommendation, or favoring by the United States Government or any agency thereof. The views and opinions of authors expressed herein do not necessarily state or reflect those of the United States Government or any agency thereof.

ABSTRACT

The University of Missouri-Rolla will identify materials that will permit the safe, reliable and economical operation of combined cycle gasifiers by the pulp and paper industry. The primary emphasis of this project will be to resolve the material problems encountered during the operation of low-pressure high-temperature (LPHT) and low-pressure low-temperature (LPLT) gasifiers while simultaneously understanding the materials barriers to the successful demonstration of high-pressure high-temperature (HPHT) black liquor gasifiers. This study will define the chemical, thermal and physical conditions in current and proposed gasifier designs and then modify existing materials and develop new materials to successfully meet the formidable material challenges.

Resolving the material challenges of black liquor gasification combined cycle technology will provide energy, environmental, and economic benefits that include higher thermal efficiencies, up to three times greater electrical output per unit of fuel, and lower emissions. In the near term, adoption of this technology will allow the pulp and paper industry greater capital effectiveness and flexibility, as gasifiers are added to increase mill capacity. In the long term, combined-cycle gasification will lessen the industry's environmental impact while increasing its potential for energy production, allowing the production of all the mill's heat and power needs along with surplus electricity being returned to the grid. An added benefit will be the potential elimination of the possibility of smelt-water explosions, which constitute an important safety concern wherever conventional Tomlinson recovery boilers are operated.

Developing cost-effective materials with improved performance in gasifier environments may be the best answer to the material challenges presented by black liquor gasification. Refractory materials may be selected/developed that either react with the gasifier environment to form protective surfaces in-situ; are functionally-graded to give the best combination of thermal, mechanical, and physical properties and chemical stability; or are relatively inexpensive, reliable repair materials. Material development will be divided into 2 tasks:

Task 1, Development and property determinations of improved and existing refractory systems for black liquor containment. Refractory systems of interest include magnesium aluminate and barium aluminate for binder materials, both dry and hydratable, and materials with high alumina contents, 85-95 wt%, aluminum oxide, 5.0-15.0 wt%, and BaO, SrO, CaO, ZrO_2 and SiC.

Task 2, Finite element analysis of heat flow and thermal stress/strain in the refractory lining and steel shell of existing and proposed vessel designs. Stress and strain due to thermal and chemical expansion has been observed to be detrimental to the lifespan of existing black liquor gasifiers. The thermal and chemical strain as well as corrosion rates must be accounted for in order to predict the lifetime of the gasifier containment materials.

TABLE OF CONTENTS

LIST OF GRAPHICAL MATERIALS

INTRODUCTION

The Tomlinson recovery boiler is the conventional technology for recovering cooking chemicals and energy from black liquor. As a potential replacement for the Tomlinson recovery boiler, black liquor gasification (BLG) technology has garnered much interest over the last two decades in the papermaking industry. The BLG technology has higher energy efficiency and generates far more power with overall lower cost than conventional technology. It improves safety by reducing the risk associated with smelt-water explosions. It reduces the wastewater discharges and harmful emissions into the environment. BLG systems recover sodium and sulfur as separate streams that can be blended to produce a wide range of pulping liquor compositions [Stigsson (1998)]. As a technique that is still under development, it has problems including refractory failure during operation due to a combined effect of chemical reaction and thermomechanical stress [Brown and Hunter (1998), Dickinson, Verrill and Kitto (1998)]. The objective of this study is to investigate the failure behavior of refractory lining under chemical and thermomechanical loading by using an analytical model.

High temperature black liquor gasifiers are generally cylindrical in shape as shown in Figure 1. The height ranges from 1.5 m to 25 m and diameter ranges from 0.5 m to 5 m. In the gasifier reactor vessels, there are usually 2-6 coaxial layers of component lining [Taber (2003)]. Refractory lining is used to protect the exterior metallic part of the gasifier vessel. A dense refractory material layer is designed to be exposed to the highest temperature environment. The second “safety” layer is usually made of a similar material. Subsequent layers are used to provide insulation and allow for expansion. The steel shell is used to provide reaction space and confinement. The gasifier generally operates at temperature ranging from 950 to 1000 ^{o}C.

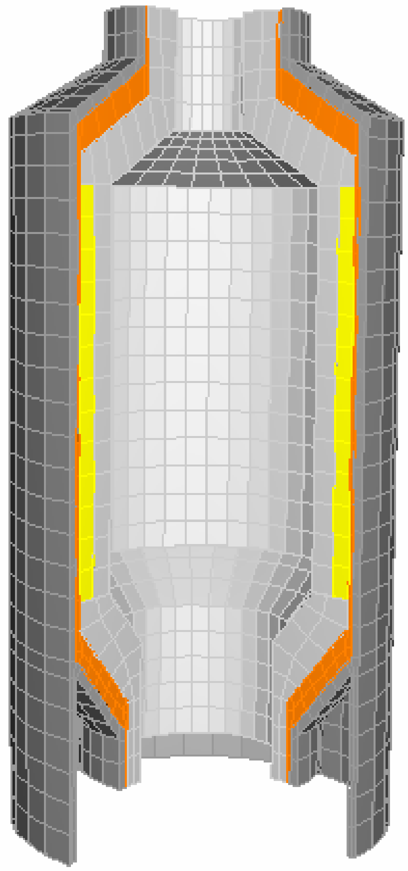

Figure 1 Schematic construction of a typical high temperature gasifier

The commercial high temperature black liquor gasifier was developed by Kvaerner Chemrec. A pilot plant first started running in 1994 at a pulp mill near Karlstad, Sweden [Larson, Consonni and Katofsky (2003)]. The first commercial size Chemrec system (75-100 tons of dry solids/day) was built at the AssiDomän mill in Frövifors in 1991. This air blown gasifier has performed well and been proven to be easy to operate and maintain. The first commercial Chemrec system in North America started operation in 1996 at Weyerhaeuser's New Bern, SC, USA [Brown and Hunter (1998)]. It was an atmospheric, air-blown, entrained bed gasifier operating between 950-1000 ^{o}C with a capacity of 350 ton black liquor solids per day. However, this system was shutdown in January 2000 due to failure of the stainless steel shell [Brown and Landalv (2001)].

Black liquor gasification converts the organic components into combustible fuel gas and leaves inorganic components as smelt to generate high-quality green liquor for regenerating pulping chemicals [Kelleher and Kohl (1986)]. The combustible gas contains carbon monoxide (CO), hydrogen (H_2), carbon dioxide (CO_2), methane (CH_4), nitrogen (N_2), water vapor (H_2O) and hydrogen sulfide (H_2S). The smelt drops are mainly sodium carbonate (Na_2CO_3) and sodium sulfide (Na_2S). Some of the smelt drops form a thin layer of smelt flowing along the reactor wall.

The current refractory materials for the BLG reactor vessel lining are not deemed adequate. The combination of high temperature and alkalinity produces an aggressive environment for the reactor lining. Chemrec has used several refractory materials in the pilot units and the commercial atmospheric units. The refractories last from 1 to 18 months, with a replacement cost of up to 1 million dollars and several weeks of downtime. Severe refractory thinning occurred and several bricks were found lost from the upper part of the gasifier vessel during operation. The refractory lining is subjected to the penetration of sodium and subsequent reactions with alkali-rich molten smelt, such that the refractory undergoes significant volume change and strength degradation. Several refractory samples have been studied after immersion in molten smelt by Peascoe, Keiser, Hubbard, Brady and Gorog (2001). The results of their study are summarized below. For mullite based refractories, molten smelt first attacks mullite and forms sodium aluminum silicates. This reaction is accompanied by a volume change. A significant surface expansion occurs during immersion testing in smelt. Furthermore, a liquid phase can develop in the mullite refractory as Na_2O concentration increases. Surface expansion coupled with the loss of structural integrity lead to the spalling of the lining. $MgAl_2O_4$ spinel based refractories react with the smelt to form $NaAlO_2$ and MgO, with an associated expansion of 2.1% to 13%. For α/β-alumina refractories, expansion was accommodated partly through spalling and a significant radial expansion of the gasifier's lining. The alumina refractories show the least corrosion, the chemical expansion of alumina samples is from 0 to 0.7%. Due to this reason, fused cast alumina which is expansive and sensitive to thermal shock is being used in the most recent commercial high temperature black liquor gasifier at New Burn, SC, USA, [Brown, Leary, Gorog and Abdullah (2004)].

Computer simulation of existing materials will accelerate the development of these new materials. Compared to experimental characterization, computer simulation is much faster and more economical. Finite element modeling of damage evolution in refractory linings exposed to high temperature and aggressive chemical environment is presented.

Due to the difficulties in describing the evolution of the micro-crack pattern in a failing brittle solid, continuum damage mechanics (CDM) has been used extensively to describe the failure processes of brittle materials such as concrete, rock and glass.

Continuum damage mechanics, regarded as a continuous measurement of the state of internal stiffness degradation of a material, was first introduced by Kachanov (1958) and further developed by Lemaitre (1985), Kachanov (1986), and Chaboche (1988). A scalar variable, D, between 0 and 1 is used to describe the damage. The constitutive law for a damaged material was derived by using the effective stress, along with the principle of strain equivalence.

The damage variable is described in terms of stiffnesses as

$$D = 1 - \frac{\tilde{E}}{E} \tag{1}$$

where $\tilde{E}$ is the elastic modulus of the damaged material, and E is the elastic modulus of the undamaged material. The effective stress, $\tilde{\sigma}$, in a damaged material under uniaxial load is then expressed in terms of D as

$$\tilde{\sigma} = \frac{\sigma}{1 - D} \tag{2}$$

where σ is the normal stress. Failure would occur when the damage, D, reaches critical damage D_c. The concept of failure here represents the formation of macroscopic defects rather than the rupture.

Hillerborg, Modeer and Petersson (1976) studied the tensile behavior of concrete and described a method that explains both the growth of existing cracks and the formation of new cracks. They proposed a fictitious-crack model based on theory of plasticity. The formation and propagation of cracks was assumed to start when the tensile stress reaches a critical value. A plastic-damage model was introduced by Lubliner, Oliver, Oller and Oñate (1989) to describe the non-linear behavior of concrete, including tensile and compressive failure. The model was further developed by Lee and Fenves (1998). In their model, isotropic damage variables were used to represents the degradation of elastic stiffness. Uniaxial tensile and compressive stresses were expressed in terms of damage and effective stress. The effective stress was related to the damaged elastic stiffness and the elastic strain. The plastic strain rate was evaluated by a flow rule, using a scalar plastic potential function.

Saetta, Scotta and Vitaliani (1998) studied the mechanical behavior of concrete under physical-chemical attacks by using a coupled mechanical and chemical damage model. The mechanical damage, D_{mech}, was defined as the ratio between the area occupied by the voids and the overall section area.

$$D_{mech} = 1 - \frac{\tilde{S}}{S} \tag{3}$$

where $\tilde{S}$ is the effective area of the damaged material and S is the overall section. Since the effective area decreases continuously, the damage variable is thus an increasing parameter.

The chemical damage, D_{chem}, is defined by

$$D_{chem} = (1-\varphi) - \frac{1-\varphi}{1+(2R)^4} \tag{4}$$

where coefficient φ is the relative residual strength of the material achieved when the chemical reaction is completely developed and the parameter R is defined as the ratio between the actual concentration and the reference concentration of the reactive media, C/C_{ref}.

By combining the mechanical and chemical damage, the coupled damage, D, is given by

$$D = 1 - (1 - D_{mech}) \cdot (1 - D_{chem}) \tag{5}$$

Then the constitutive relation for the damaged material is given in terms of D as

$$\sigma_{ij} = (1 - D) \cdot E^0_{ijkl} \cdot \varepsilon_{kl} \tag{6}$$

where σ_{ij} and ε_{ij} are the standard stress and strain tensors and E^0_{ijkl} is the elastic constitutive tensor.

Refractory materials exhibit brittle behavior at low temperature, but behave in a ductile manner at high temperature [Schacht (1995)]. The knowledge on the failure behavior of refractory materials exposed to high temperature and chemical corrosive environments is very sketchy at the present time. Some investigators [Buyukozturk and Tseng (1982), Chen (1990), Boisse, Gasser and Rousseau (2002)] have used the material models of concrete to evaluate the behavior of refractory lining. This approach may be appropriate for evaluating the stress-strain behavior of refractories. However, serious concerns exist when those models are used to analyze failure of refractory materials [Chen (1990) and Schacht (1995)]. The concrete material shows an orthotropic and non-linear inelastic behavior which is not true for refractory materials. The structural concrete is typically exposed to ambient temperature, but the refractory materials operate at high temperatures and in a severe chemical corrosive environment.

In this study, the refractory material is assumed to be continuous, homogeneous and isotropic. Due to the ductile behavior of refractory at high temperature and the irreversible reactive strain due to the chemical attack, the plastic strain and chemical reactive strain also need to be included in the analysis in addition to the elastic strain.

The total strain ε is the sum of the mechanical strain ε^m, thermal strain ε^t and reactive strain ε^r. It is also equal to the sum of elastic strain ε^e and inelastic strain ε^i. The inelastic deformation consists of the plastic strain and the reactive strain, so that

$$\varepsilon = \varepsilon^m + \varepsilon^t + \varepsilon^r = \varepsilon^e + \varepsilon^i \tag{7}$$

The chemical reaction is assumed to be continuous and linearly related to the temperature T and time t. The reactive behavior of refractory material is expressed by the reactive strain which is proportional to temperature and time as

$$\varepsilon^r = F(T,t) \tag{8}$$

A continuum, plasticity-based, damage model is used to study the failure behavior for the refractory material. It consists of the combination of non-associated, multi-hardening plasticity and isotropic damaged elasticity to describe the irreversible damage that occurs during the fracturing process. The dominant failure mechanisms are tensile cracking and compressive crushing of the refractory material.

The evolution of the failure surface is controlled by two hardening variables, $\tilde{\varepsilon}_t^i$ and $\tilde{\varepsilon}_c^i$, linked to failure mechanisms under tension and compression loading, respectively. $\tilde{\varepsilon}_t^i$ and $\tilde{\varepsilon}_c^i$ are referred to as tensile and compressive equivalent inelastic strains, respectively.

It is assumed that the tensile and compressive response of refractory material is characterized by damaged plasticity, as shown in Figure 2. Under tension, the stress-strain response follows a linear elastic relationship up to the failure stress, σ_t^f, which corresponds to the initiation of micro-cracking. Beyond the failure stress, the formation and propagation of micro-cracks are represented with a softening stress-strain response. Under compression, the response is linear up to the initial yield, σ_c^f. In the plastic regime the response is typically characterized by hardening up to the ultimate stress, σ_c^u followed by softening.

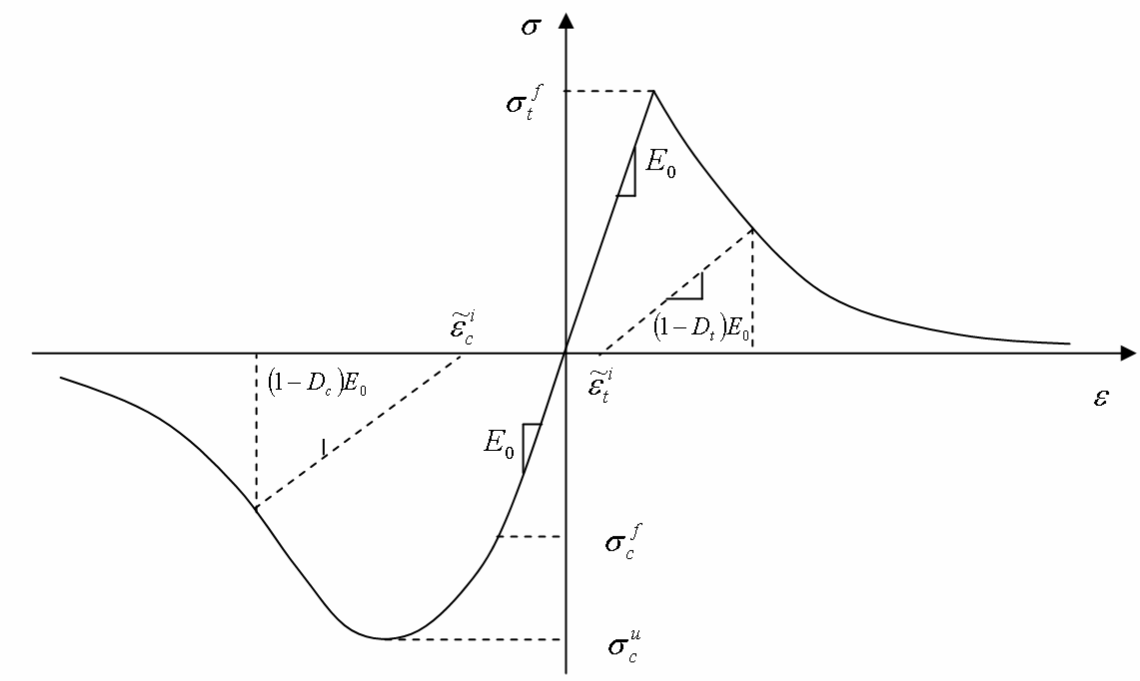

Figure 2 Response of refractory material to loading in tension and compression

Based on the model of Lee and Fenves (1998), it is assumed that the stress-strain relations can be converted into stress- inelastic-strain relations as

$$\sigma_t = \sigma_t\left(\tilde{\varepsilon}_t^i, \dot{\tilde{\varepsilon}}_t^i, T\right) \tag{9}$$

$$\sigma_c = \sigma_c\left(\tilde{\varepsilon}_c^i, \dot{\tilde{\varepsilon}}_c^i, T\right) \tag{10}$$

where σ_t and σ_c are tensile and compressive stresses, respectively, $\tilde{\varepsilon}_t^i$ and $\tilde{\varepsilon}_c^i$ are the equivalent inelastic strains, $\dot{\tilde{\varepsilon}}_t^i$ and $\dot{\tilde{\varepsilon}}_c^i$ are the equivalent inelastic strain rates and T is the temperature.

Due to internal damage, the elastic stiffness of the material degrades. The degradation of the elastic stiffness is characterized by tensile and compressive damage variables, D_t and D_c, which are assumed to be functions of the inelastic strains and temperature as

$$D_t = D_t\left(\tilde{\varepsilon}_t^i, T\right); \quad 0 \le D_t \le 1 \tag{11}$$

$$D_c = D_c\left(\tilde{\varepsilon}_c^i, T\right); \quad 0 \le D_c \le 1 \tag{12}$$

The corresponding stress-strain relations under tension and compression loading are

$$\sigma_t = (1 - D_t)E_0\left(\varepsilon_t - \tilde{\varepsilon}_t^i\right) \tag{13}$$

$$\sigma_c = (1 - D_c)E_0\left(\varepsilon_t - \tilde{\varepsilon}_c^{\,i}\right) \tag{14}$$

where E_0 is the initial (undamaged) elastic stiffness of the material.

Now the effective tensile and compressive stresses can be defined as

$$\tilde{\sigma}_t = \frac{\sigma_t}{(1 - D_t)} = E_0\left(\varepsilon_t - \tilde{\varepsilon}_t^{\,i}\right) \tag{15}$$

$$\tilde{\sigma}_c = \frac{\sigma_c}{(1 - D_c)} = E_0\left(\varepsilon_c - \tilde{\varepsilon}_c^{\,i}\right) \tag{16}$$

EXECUTIVE SUMMARY

Black liquor gasification is a high potential technology for production of energy which allows substitution for other sources of energy. This process uses a waste of the pulp and paper industry as black liquor to produce synthetic gas and steam for production of electricity; therefore development of this technology not only recovers the waste of the paper industry but also decreases dependency on fossil fuel.

Today one of the main obstacles in the development of this technology is the development of refractory materials for protective lining of the gasifier. So far the materials used for this application have been based on alumino-silicate refractories but, thermodynamics and experience shows that these materials are not sufficiently resistant to black liquor under the harsh working conditions of Black liquor gasifiers. Consequently development of cost-effective materials with improved performance in gasifier environments to answer the material challenges presented by black liquor gasification (HTHP, HTLP) is the objective of this project. Refractories provided by in-kind sponsors were tested by cup testing, density/porosity determinations, chemical analysis and microscopy. The best performing materials in the cup testing were fused cast materials. Currently testing of 2 castables are being completed and 1 magnesia brick. These appear to be outperforming any of the previously tested materials.

Computer simulation of existing materials will accelerate materials research in developing these new materials, and it is less costly and time consuming. Finite element modeling was conducted for the damage analysis in this study.

This study presented continuum damage mechanics based on analytical model for predicting the failure behavior of refractory lining in high temperature black liquor gasifiers. The damage model accounts for the chemical expansion in addition to mechanical and thermal expansion. A comparison of predicted damage patterns for BLG refractory material with the observed damage pattern in a glass melting furnace refractory brick indicates that this model could be used to evaluate failure behavior of refractory linings in black liquor gasifier.

Chemical reaction causes the most compressive damage in the refractory structure. Layered damage occurred in the refractory structure due to the tensile damage. Expansion allowance affects the damage of the refractory structure. Tensile damage could be reduced by allowing for larger expansion. Compressive damage is not dependent on the expansion allowance provided by the fiber layer.

No systematic experimental work has been done so far to characterize the failure behavior of refractory materials in black liquor gasifier. Experimental work is needed to validate the damage model presented here.

EXPERIMENTAL

Cup testing has been used for the preliminary determinations of smelt refractory reactions for Task 1.3. Cup test processing was performed at UMR. Cups were prepared from monolithic materials according to the manufacturers directions as a 9" long by 4.5" wide by 3" deep sample with 2 of 1.5" diameter by 1.5" deep holes formed during casting. Brick samples were cut from a 9 inch straight into 2 of 4.5 inch by 4.5 inch by 2.5 inch specimens. A diamond core drill cored a 1.5" diameter by 1.5" deep core. The core was removed with a chisel.

The removed cores were used to determine density by ASTM C-830-00 and sectioned for chemical analysis by ICP and microscopy. The cups are processed by drying at 110°C for 24 hours. The cup was charged with 50 grams of raw black liquor smelt. Heated at 1°C/minute to 1000 °C, held 240 hours at 1000°C and cooled at 1°C/minute to 25 °C, in an argon flooded furnace.

Commercial finite element software ABAQUS® by Hibbitt, Karlsson & Sorensen, INC. (2002) is used for the modeling. The model is composed of two layers of refractory lining, one layer of fiber and finally the steel shell. Because of axisymmetry, each layer of refractory lining consists of only one-half of a brick. One side of the half brick model is the centerline of the brick and the other side corresponds to the brick joint as shown in Figure 3. Since dry joints are used in the model, the brick joint will open under tensile stress. The outer diameter of the reactor is 3 m. The thicknesses of each alumina refractory layer is 152 mm; the thickness of the carbon steel shell is 30 mm; and two different thicknesses, 10 mm and 20 mm are considered for the fiber layer between the second refractory layer and the steel shell.

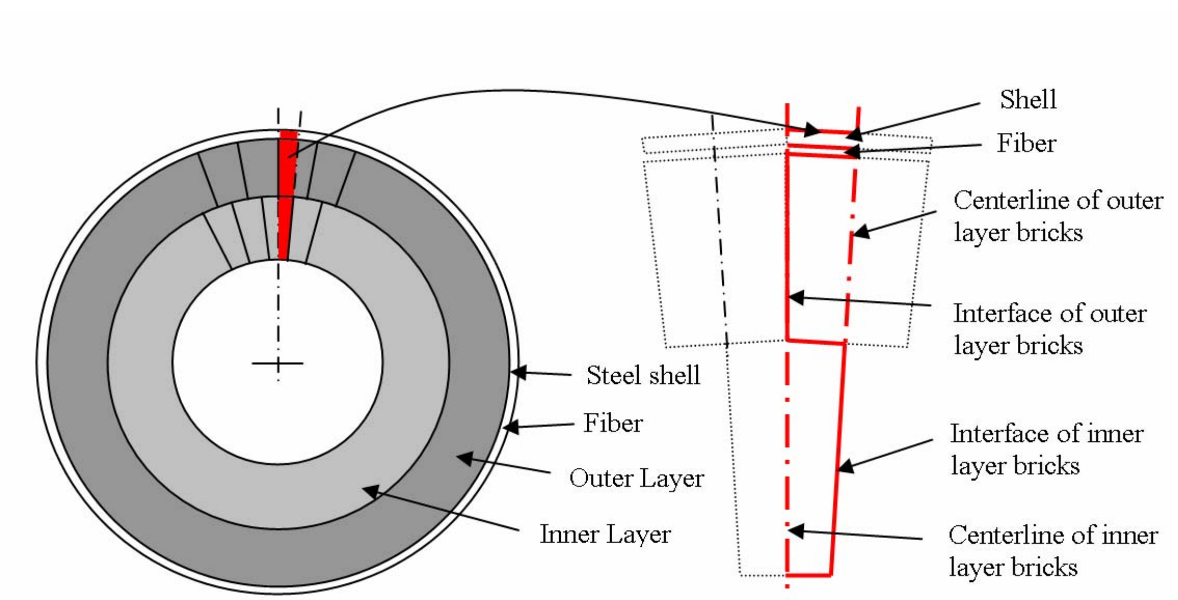

Figure 3 Illustration of the modeled part in black liquor gasifier

The thermal and mechanical properties of the refractory material are temperature dependent. The alumina refractory material is simulated as elastic-plastic material. Temperature dependent thermal and mechanical properties of the refractory are given in Table 1 based on the study of Hemrick (2001). Linear elastic properties are used for steel. Among these, Young's Modulus is 210 GPa, Poisson's ratio is 0.3, density is 7800 kg/m^3, thermal conductivity is 55 W/mK, specific heat is 500 J/gK, thermal expansion coefficient is 13 x 10^{-6} and the emissivity is 0.8. A fiber material which could be compressed up to 80% in volume (Figure 4) is used in the model based on industrial practices [Brown, Leary, Gorog and Abdullah (2004)]. Simple temperature independent thermal and mechanical material properties for the fiber material are used due to the lack of data. These are Density = 300 kg/m^3, thermal conductivity = 0.2 W/mK, specific heat = 2900 J/gK and negligible thermal expansion. In the areas where the experimental evidence was not conclusive, the general knowledge of the behavior of conventional material was employed to idealize the material behavior.

Table 1 Temperature dependent properties of alumina used in the model [Hemrick (2001)]

Temperature (°C)	Thermal conductivity (W/m K)	Specific heat (J/g K)	Density (kg/m^3)	Coefficient of thermal expansion 10^6 (1/K)	Elastic Modulus (GPa)	Poisson's ratio
23	9.34	778	3480	8.70	103	0.24
100	9.28	916	--	--	--	--
200	8.29	1010	--	--	--	--
300	7.55	1080	--	--	--	--
400	6.75	1130	--	--	--	--
500	5.81	1170	--	--	--	--
600	4.37	1210	--	--	--	--
700	4.65	1220	--	--	--	--
800	4.76	1240	--	--	--	--
900	4.86	1250	--	--	81	--
1000	5.21	1270	--	--	--	--

-- No data available

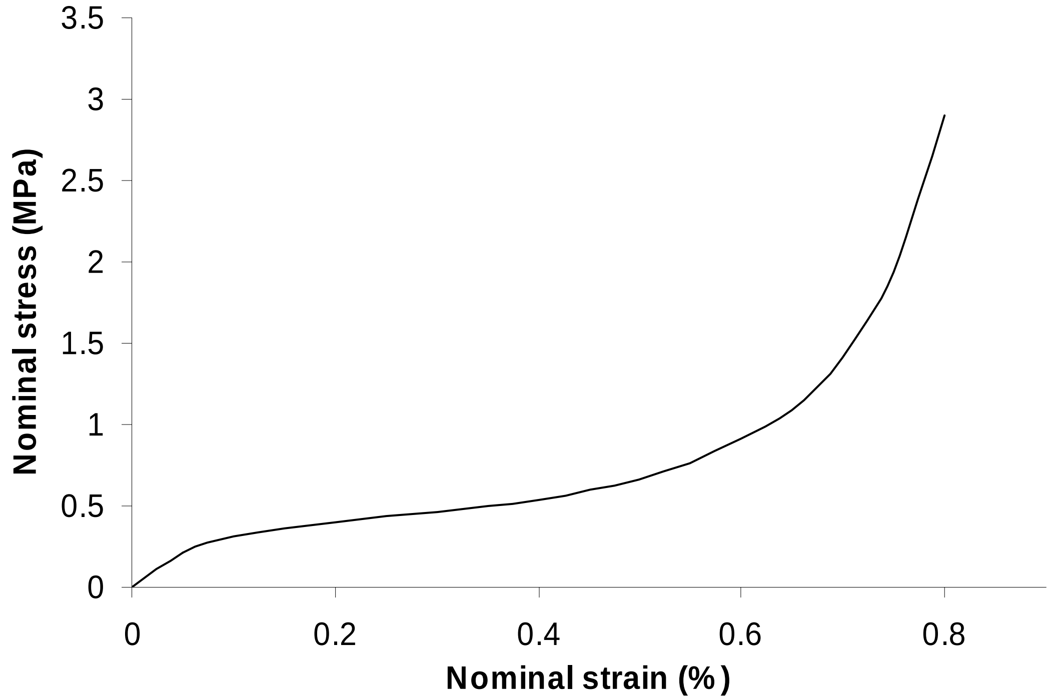

Figure 4 The compression behavior of fiber material

Strength data for commonly used alumina refractories can be found from some online database systems [Matweb.com and NIST]. The ambient temperature compressive and tensile strengths of alumina are about 3000 MPa and about 200 MPa, respectively. Even though it is well known that the strength of refractory materials would be decreased dramatically when exposed to high temperature and chemical attack, no experimental work has been done to characterize this behavior. Due to the paucity of knowledge on the behavior of refractories under chemical attack, assumptions need to be made for damage characterization of refractory materials. Lower critical compressive and tensile strengths of 200 MPa and 50 MPa are used. In order to obtain more realistic results from the analysis, experimental studies need to be carried out to define the failure behavior of refractory materials under high temperature and corrosive environments.

The gasifier is considered to be a long hollow cylinder with composite walls heated from the centerline uniformly along the axis. The temperature distribution is considered to vary in the radial direction only. The reactor is heated up to 950 ^{o}C and the heat is conducted through the wall and dissipated by radiation and convection from the outside shell surfaces to the surrounding medium. The external atmospheric temperature, the coefficient of the convection, and the heating rate are 49 ^{o}C, 30 W/m^{2} K and 20 ^{o}C/h, respectively.

The thermal and mechanical behaviors are coupled. The swelling due to chemical reaction during operation is also coupled with thermal expansion. A coupled temperature-displacement analysis is conducted using the FEA model. A user defined expansion model including the thermal expansion and the reactive expansion was implemented into the global model.

RESULTS AND DISCUSSION

Task 1.3

Samples of currently used , in-house, and refractories developed based on the results provided previously were provided by in-kind sponsors. These samples were tested according to the experimental procedure given.

The best performing materials in the cup testing were fused cast materials. Testing of 2 castables were completed and 1 magnesia brick. These appear to be outperforming any of the previously tested materials. 4 new magnesia castables were developed by a cost share partner and submitted for testing. They plan to submit one to two more during the project.

A company provided two castable refractories materials, 25 and 26 to UMR for cup testing with black liquor smelts (high alkali content).

Sample: 25

Type: Castable

Chemistry: Al_2O_3 78.2%, SiO_2 18.1%, Fe_2O_3 1.4%, TiO_2 1.9%, CaO 0.1%,
MgO 0.1%, Alk. 0.2%, P_2O_5, SiC, ZrO_2, Other.

Density: 2.69 g/cc

Porosity: 14.98%

Notes:

Sample: 26

Type: Castable

Chemistry: Al_2O_3 84.0%, SiO_2 7.5%, Fe_2O_3 0.1%, TiO_2 0.0%, CaO 0.2%,
MgO 8.0%, Alk. 0.2%, P_2O_5, SiC, ZrO_2, Other.

Density: 3.02 g/cc

Porosity: 14.91%

Notes:

Cup Preparation:

Casting

25: 5.8% water was used, and the mixture is easy to cast.

26: 4.6% water was used, and the mixture is easy to cast.

Firing

All two cups were fired at 1050 °C for 5 hr. The heat rate was 1 °C/min. The cooling rate was also 1 °C/min.

Charge smelt

50 g smelt was charged to each cup.

Two cups were set in the box furnace. The furnace was flooded with Argon gas. The test temperature was 1000 °C. The test time was 240 hr. the heat and cooling rate were 1 °C/min.

Both cups have good resistance against smelts attack. Figure 5 shows the top view of sample 25 after cup test with 50 g smelts at 1000 °C for 240 hr. Figure 6 shows the cross-section in which there is an aerage thickness of 2.3 mm corrosion ply formed.

Figure 7 shows the top view of sample 26 after cup test with 50 g smelts at 1000 °C for 240 hr. Figure 8 shows the cross-section in which there is no corrosion ply observed.

Figure 5 Top view of sample 25 after cup test.

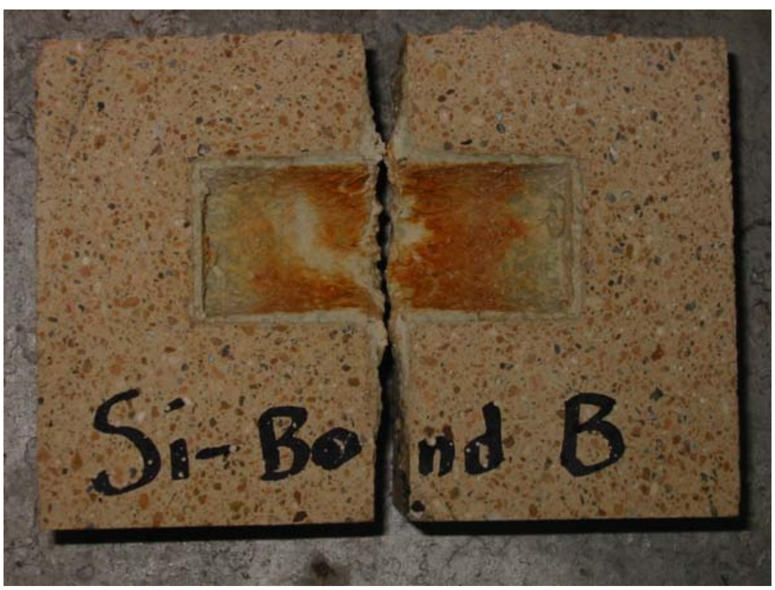

Figure 6 Cross-section of sample 25 after cup test.

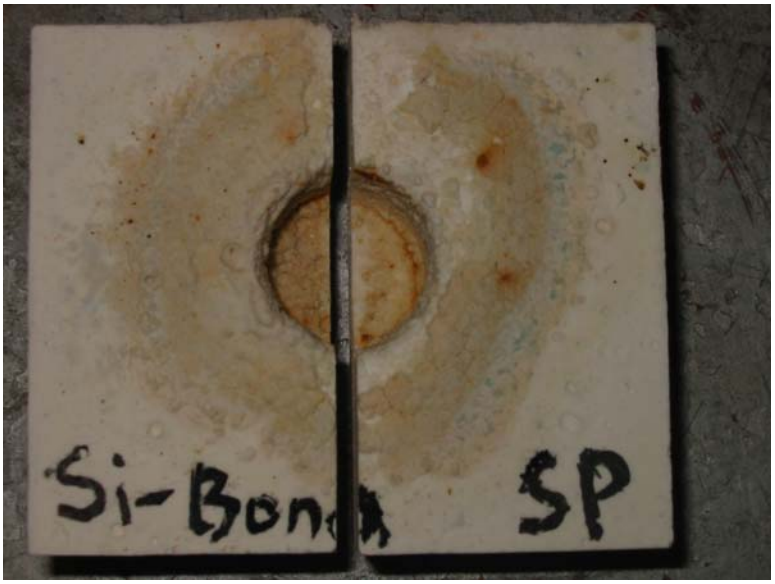

Figure 7 Top view of sample 26 after cup test.

Figure 8 Cross-section of sample 26 after cup test.

Figure 9 shows RL and CL microstructures of virgin sample 25 before firing. This sample is identified as cement-free high alumina castable refractory, which is made up of large alumina aggregates (AA), medium-sized fused mullite (FM) grains blended with most likely microsilica matrix. No calcium aluminate cement particle is identified. Alumina aggregates are highly impure containing Fe-Ti oxides as well as alkali matrix suggesting they are derived from clay-balls or bauxitic raw materials.

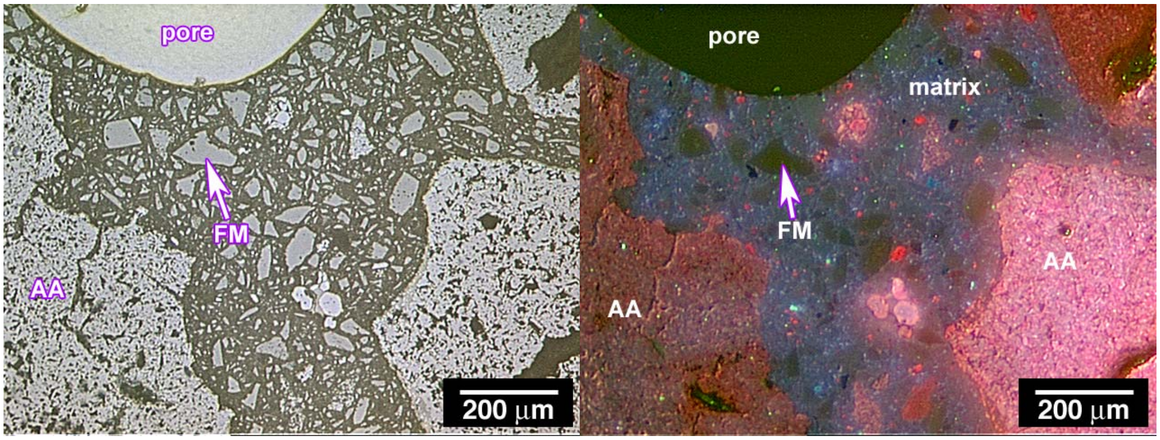

Figure 9 Pre-test microstructure for sample 25.

Figure 10 has same descriptions as in Figure 9

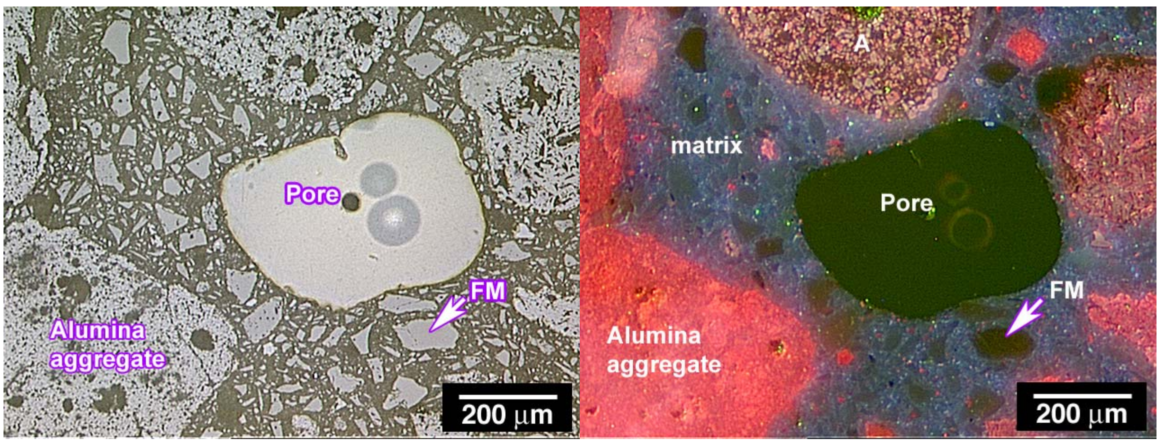

Figure 10 Pre-test microstructure for sample 25.

In Figure 11, RL/CL microstructures of sample 25 after BL smelt cup test showing reaction front. About 2 mm thick reaction interface is visible on the surface of this sample. BL smelt has reacted with refractory material to form mullite and alkali rich silicate glass.

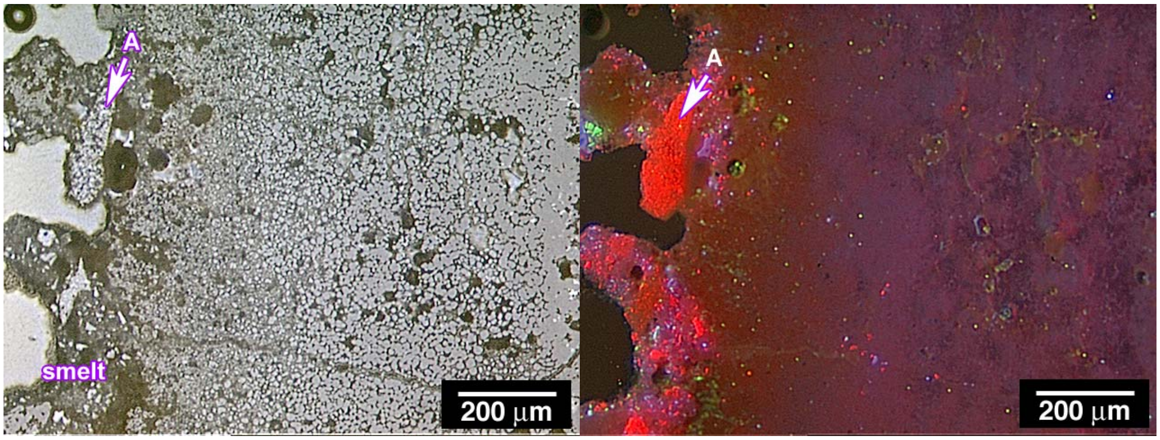

Figure 11 Post-test microstructure for sample 25.

In figure 12, these micrographs are also taken from sample 25 (adjacent to above micrographs) showing refractory-smelt interface. A dense layer is formed at the interface, which blocked further penetration of smelt. Although, this refractory altered relatively more intense compared to sample 26, the alteration is still not too intense or strong.

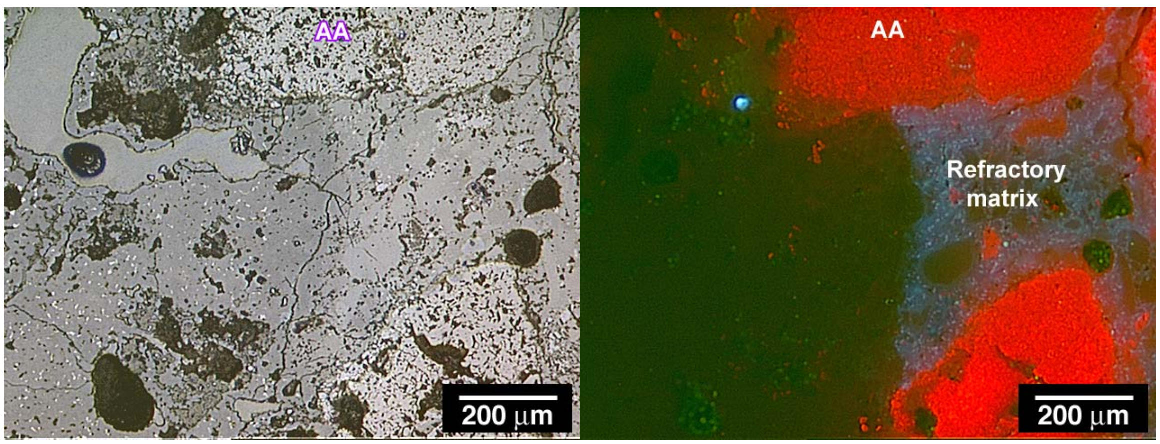

Figure 12 Post-test microstructure for sample 25.

Figure 13 shows RL/CL microstructure of sample 25 after cup test, showing interface between refractory and smelt. The thickness of alteration is negligible.

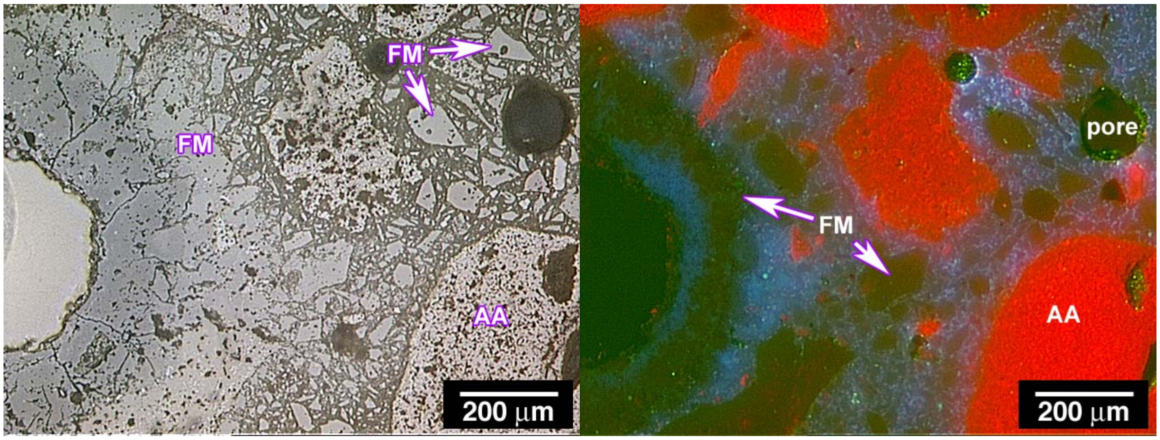

Figure 13 Post-test microstructure for sample 25.

Figure 14 shows RL and CL microstructure of virgin sample 26 before firing, which is identified as cement-free, spinel reinforced high alumina castable refractory, which contains large tabular alumina aggregates (TA), medium sized fused spinel (FS) grains, blended with most-likely microsilica (?). No calcium aluminate cement particles are identified.

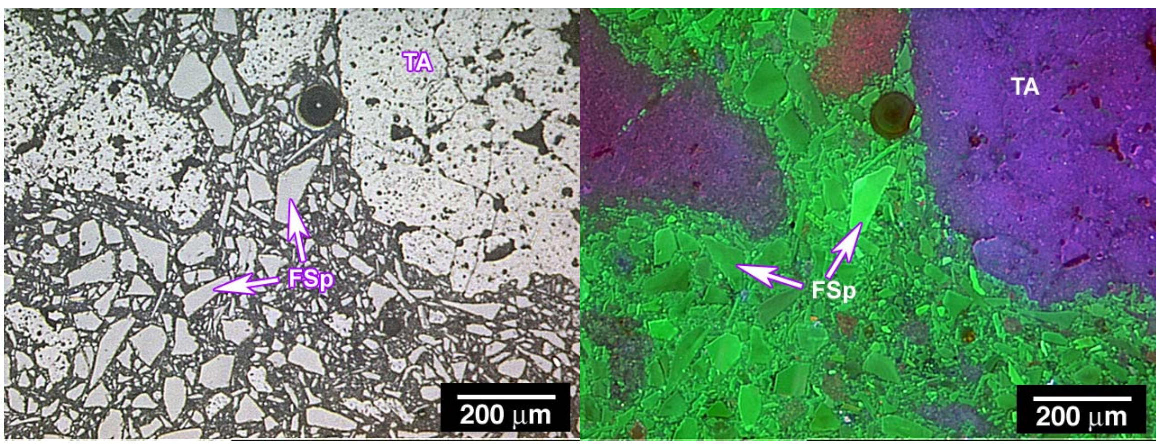

Figure 14 Pre-test microstructure for sample 26.

Figure 15 shows the same sample under low magnification showing general structure of the refractory.

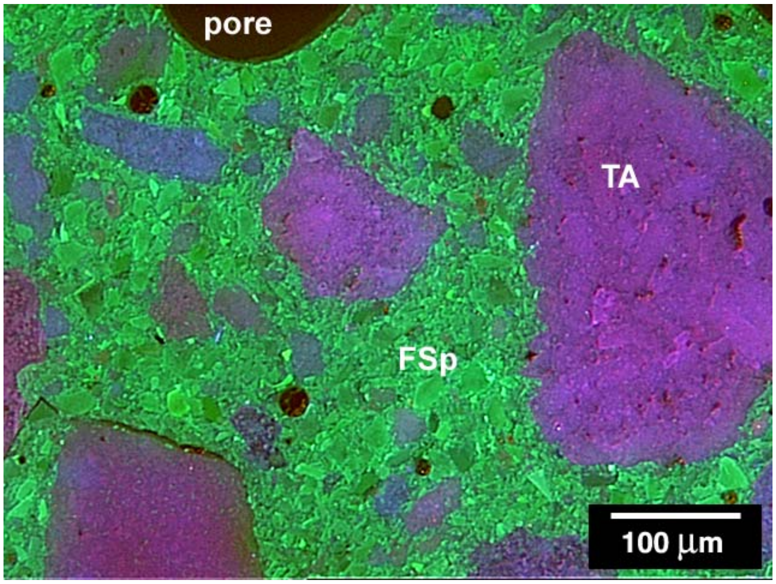

Figure 15 Pre-test microstructure for sample 26.

Figure 16 shows RL and CL micrographs taken from sample 26 after cup test, illustrating microstructure of smelt-refractory interface. Note that there is almost no smelt penetration and reaction at the interface.

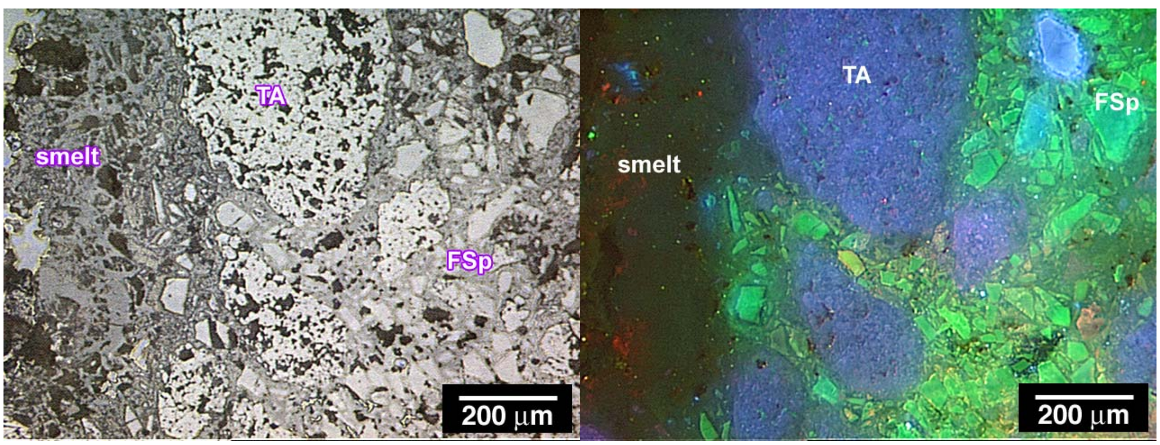

Figure 16 Post-test microstructure for sample 26.

Figure 17 shows RL and CL microstructures of sample 26 taken from refractory-smelt contact surface. Micrographs show that there is no sign of refractory degradation, for example reaction of refractory grains with smelt to form intermediate phases, in this given experimental conditions.

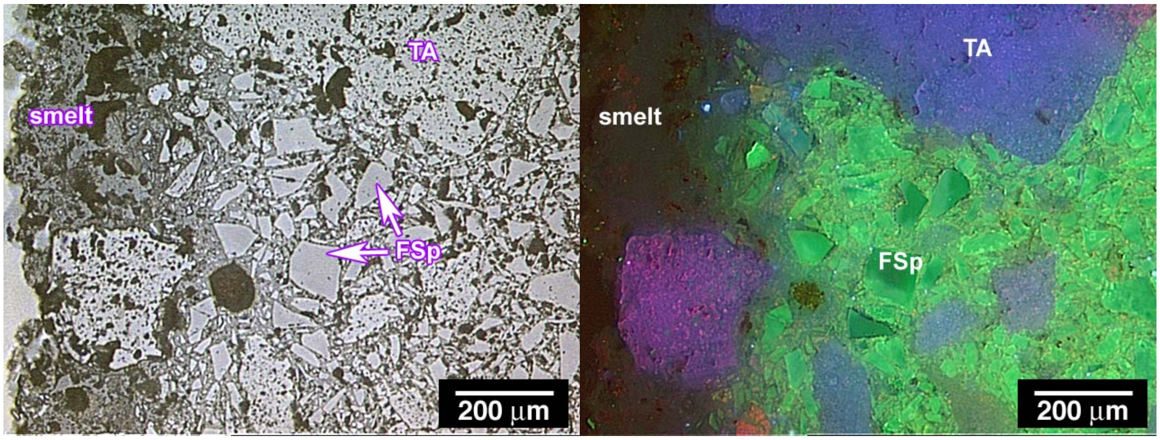

Figure 17 Post-test microstructure for sample 26.

Both 25 and 26 refractory have good corrosion resistance against smelts attack. Results indicate the 26 material is better to against smelts attack than 25.

Task 2.0

The operational environment of the outer refractory layer is much less severe than that of the inner layer. A preliminary analysis showed negligible damage in the outer refractory layer. Therefore, only the results for the inner refractory layer will be presented in the following sections.

The compressive and tensile damage patterns of refractory lining with 10 mm fiber layer are given in Figure 18. Dark color means higher damage and light color means less damage.

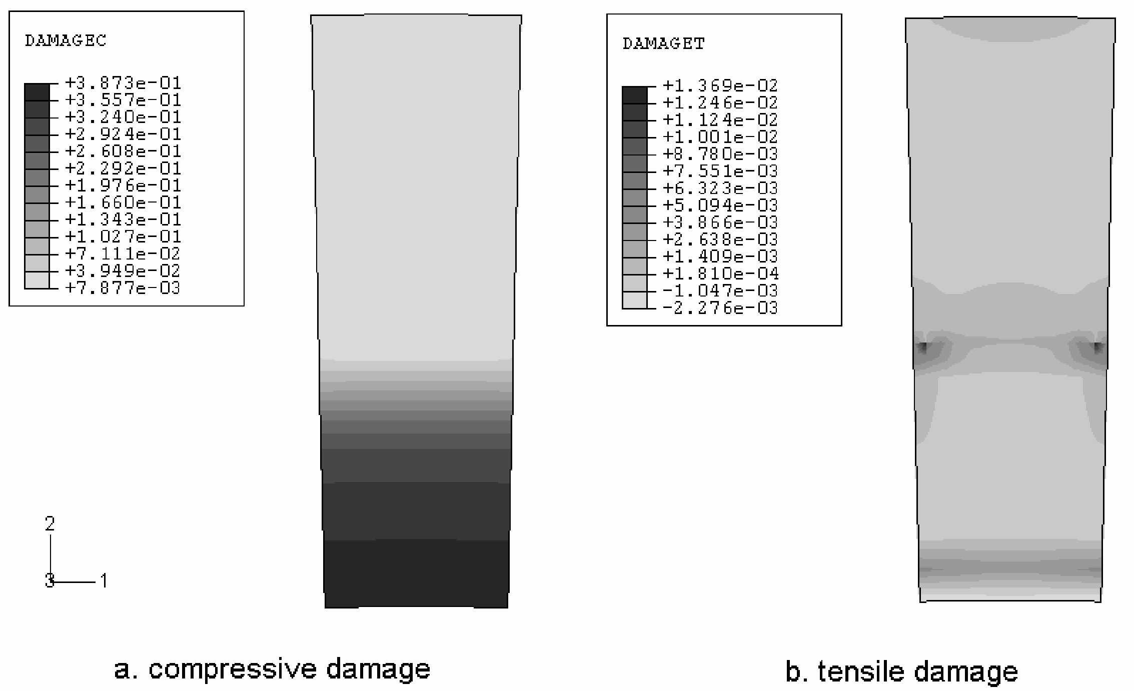

Figure 18 Damage of the refractory lining with 10 mm fiber layer after 3 months

High compressive damage occurs in the high temperature region of the inner layer refractory material. The highest compressive damage is 0.39. Tensile damages occurred near the hot face and the region about 1/3 of the total thickness of inner refractory layer from the hot face. The highest tensile damage is 0.014. The failure here does not mean fracture but rather refers to the formation of micro-cracks. As discussed before, no experimental data is yet available for the damage parameters. Therefore, the results of this study should be treated in a qualitative sense and should only be used to study the possible trends in refractory structures in real situations. A brick sample taken from a glass melting furnace, which has been exposed to similar environments as the black liquor gasifier, is shown in Figure 19 for comparison. The comparison of damage patterns predicted for BLG refractory and the observed damage pattern for glass melting furnace refractory is encouraging. From this point of view, the model presented here may be appropriate for evaluating the failure behavior of the refractory structure.

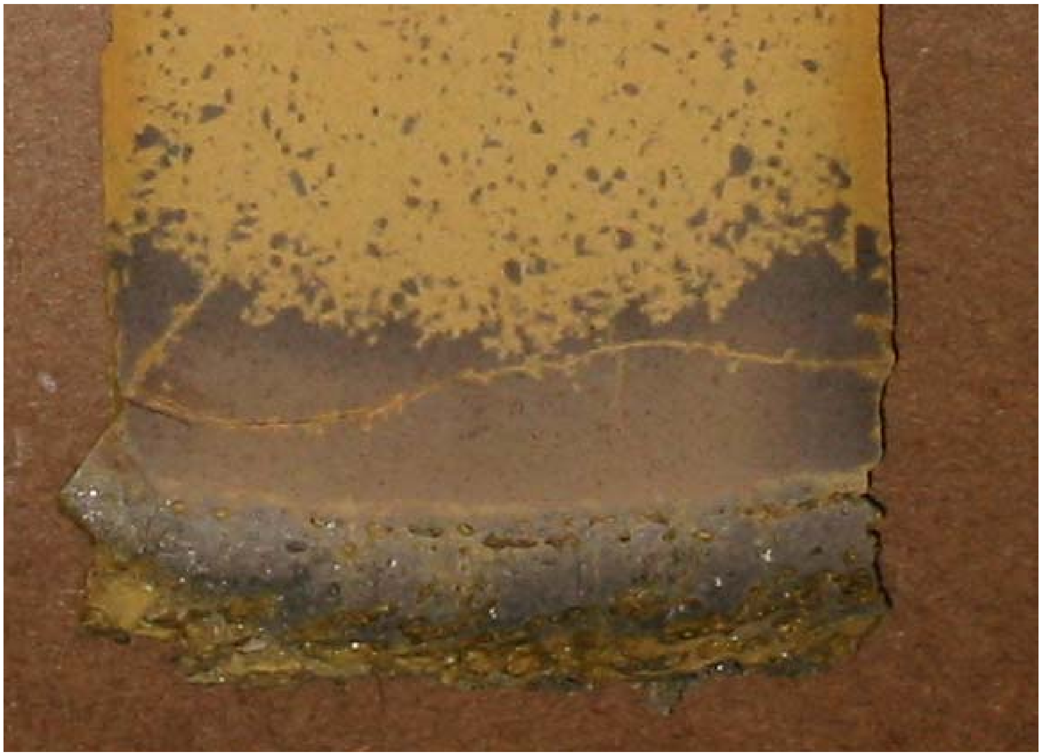

Figure 19 Damage observed in a silica brick taken from a glass melting furnace

The fiber layer plays an important role in the black liquor gasifier. It provides expansion allowance for the refractory linings and insulation for the structure. Thickness of the fiber layer affects the behavior of the refractory lining. Insufficient expansion allowance (thin fiber layer) would produce significant stresses in the refractory structure and therefore damage the refractory material. Excessive expansion allowance (thick fiber layer) would not provide enough confinement to the refractory linings, thereby resulting in an unstable lining structure. Effects of the fiber layer thickness are also studied.

The compressive and tensile damage patterns for the refractory lining with 20 mm fiber layer are given in Figure 20. The compressive damage is similar to that of the lining with 10 mm fiber layer. Only one slabbing damage pattern is found in the lining with 20 mm fiber layer. It is clear from the results that fiber thickness has little effect to the compressive damage, however, it affects the tensile damage of the refractory lining.

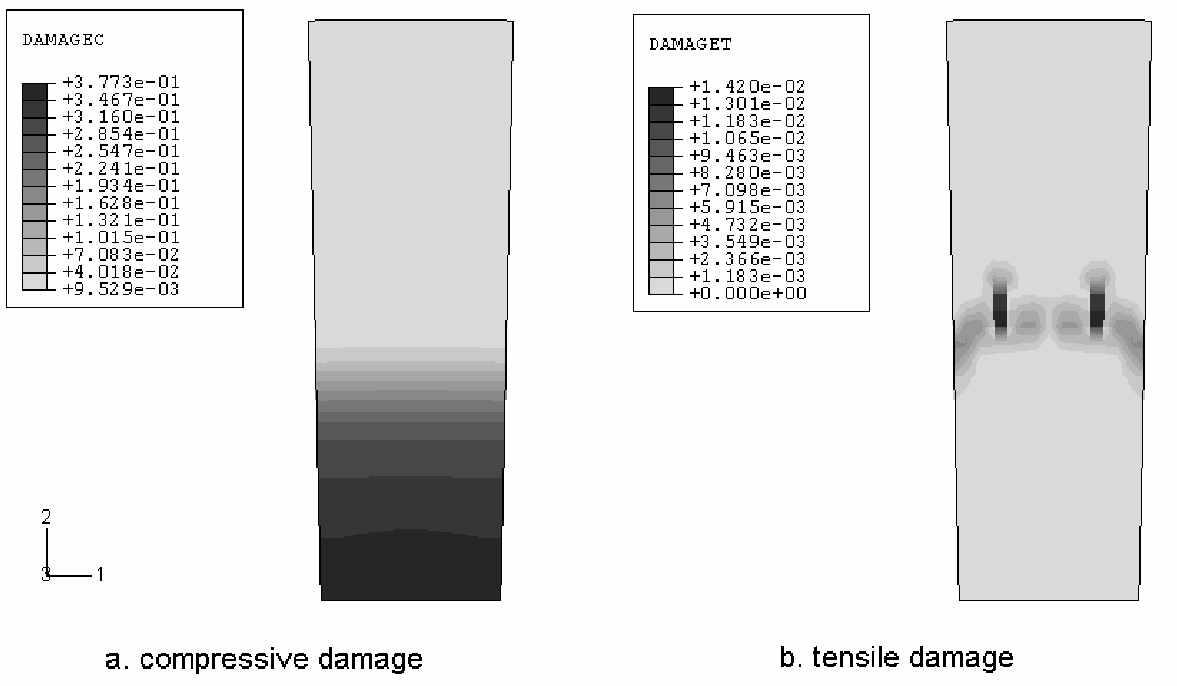

Figure 20 Damage of the refractory lining with 20 mm fiber layer after 3 months

The through thickness compressive and tensile damage for the refractory lining is given in Figures 21 and 22, respectively. The compressive damages in the two linings with different fiber layer thicknesses are almost the same. The compressive damage is maximum at the hot face and decreases with a steep gradient from the refractory hot face to the region about 50 mm from hot face where the expansion is dominated by the chemical reaction. In the other word, the reactive strain causes the most damage in the refractory. The damage curve decreased with a much higher gradient after the first 25 mm from the hot face of the refractory. This may have been caused by the separation of the refractory bricks. The opening provides an increased space for the expansion of the refractory lining, thereby causing a decreased compressive stress and subsequentially reducing the damage. The through thickness tensile damage along the centerline of the inner layer brick (Figure 22) shows a layered damage occurs in the refractory lining with 10 mm fiber layer. The damages are located occur near the hot face area and at the end of reaction zone. Only one damage region is developed in the lining with 20 mm fiber layer due to larger expansion allowance. The damage is located at the end of the reaction zone

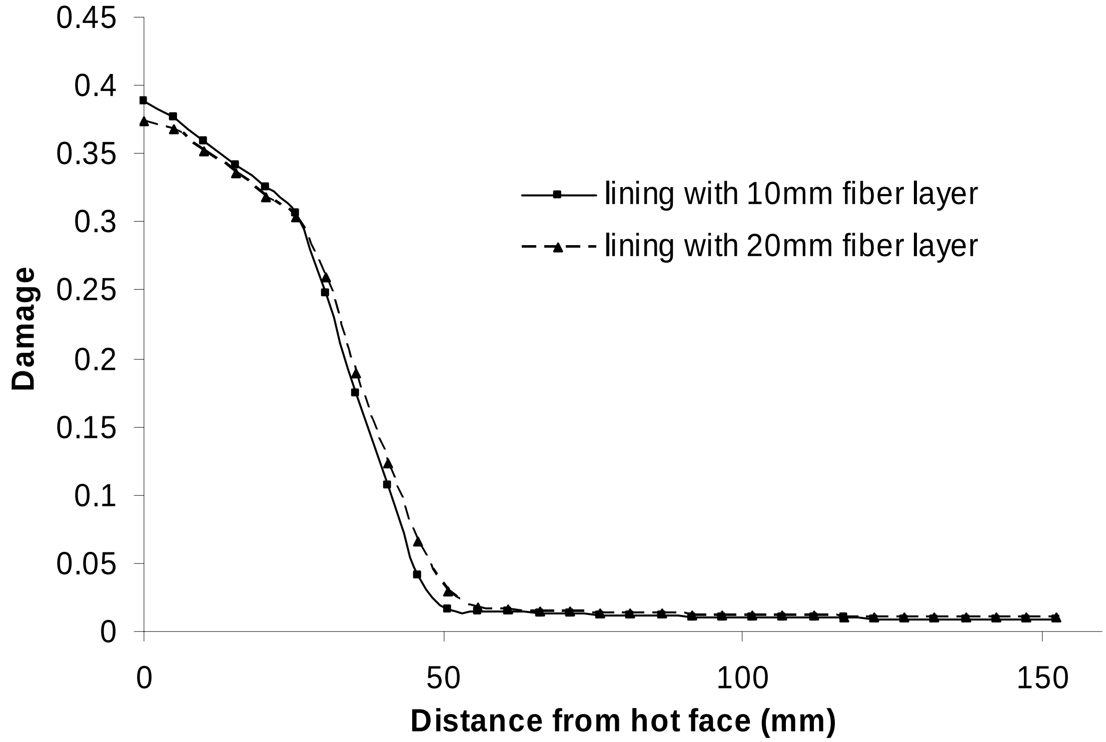

Figure 21 Through thickness compressive damage for two fiber layer thicknesses

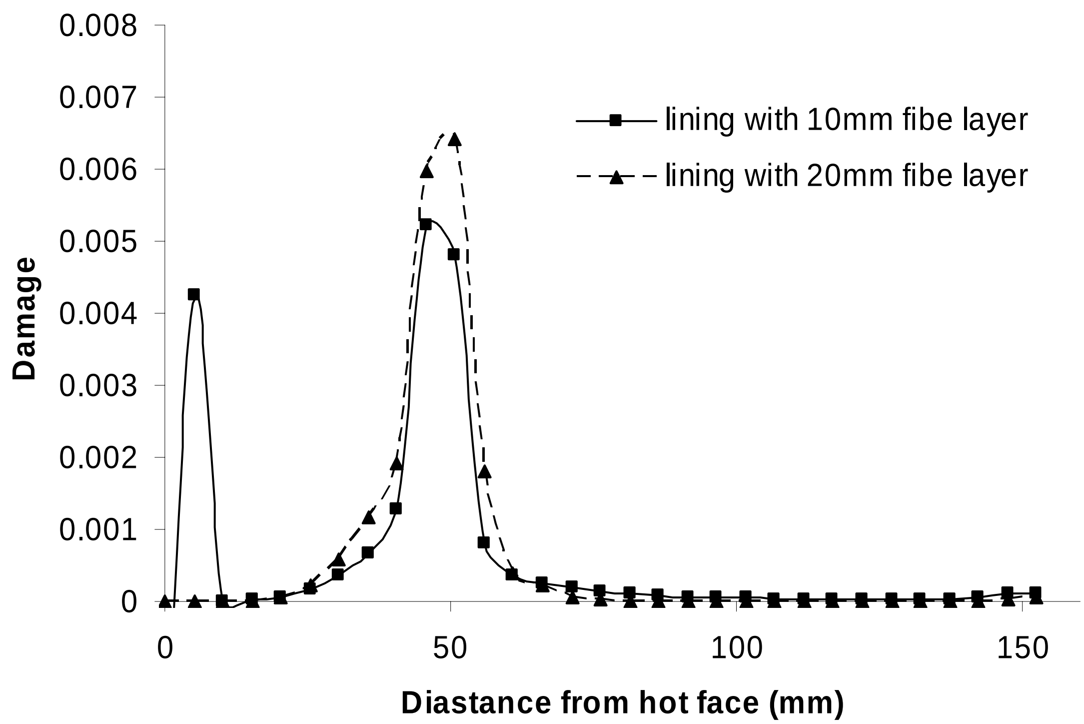

Figure 22 Through thickness tensile damage for two fiber layer thicknesses

The compressive and tensile damage histories for a 3-month time span are given in Figure 23 and Figure 24, respectively. The compressive damage shows a linear dependence on time. Since the damage was assumed to depend linearly on the chemical reaction, this result reinforces the earlier observation that the compressive damage is primarily caused by reaction strain. The compressive damage of the refractory linings with 10 mm and 20 mm fiber layers were almost the same numerically. The tensile damage-time relationship is non-linear. Most tensile damage occurs during the first 200 to 300 hours. When the fiber layer is compressed to the highest capacity of compression, the confinement from the steel shell limits the increase in the tensile deformation. A systematic experimental study is needed before one can give a phenomenological explanation of the damage process.

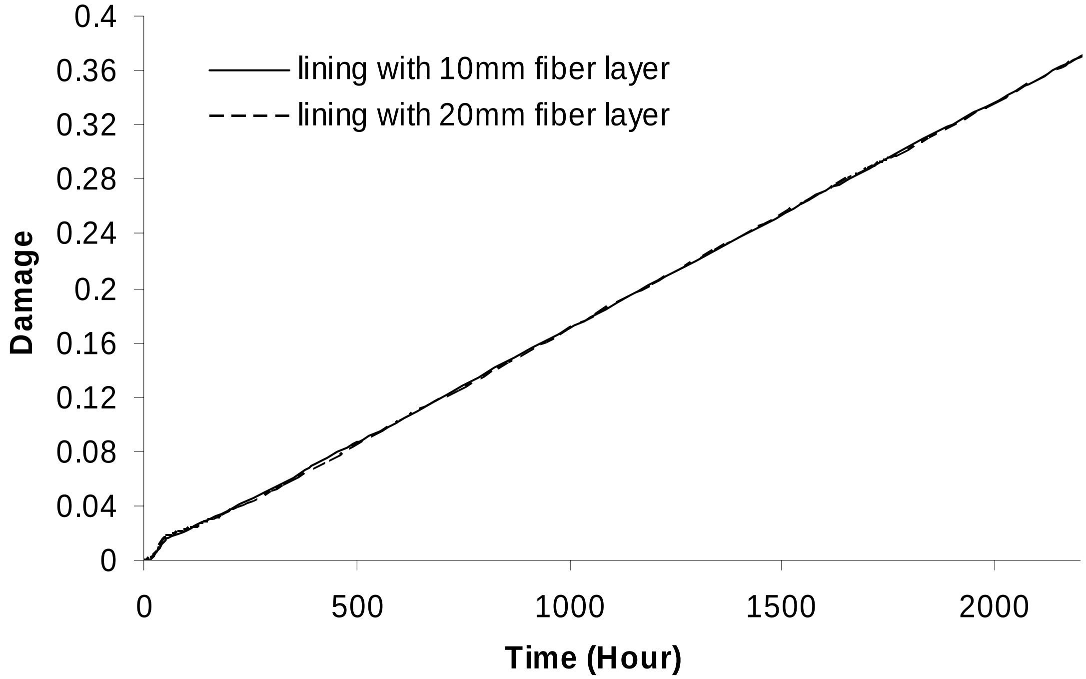

Figure 23 Compressive damage history in the refractory structure for two fiber layer

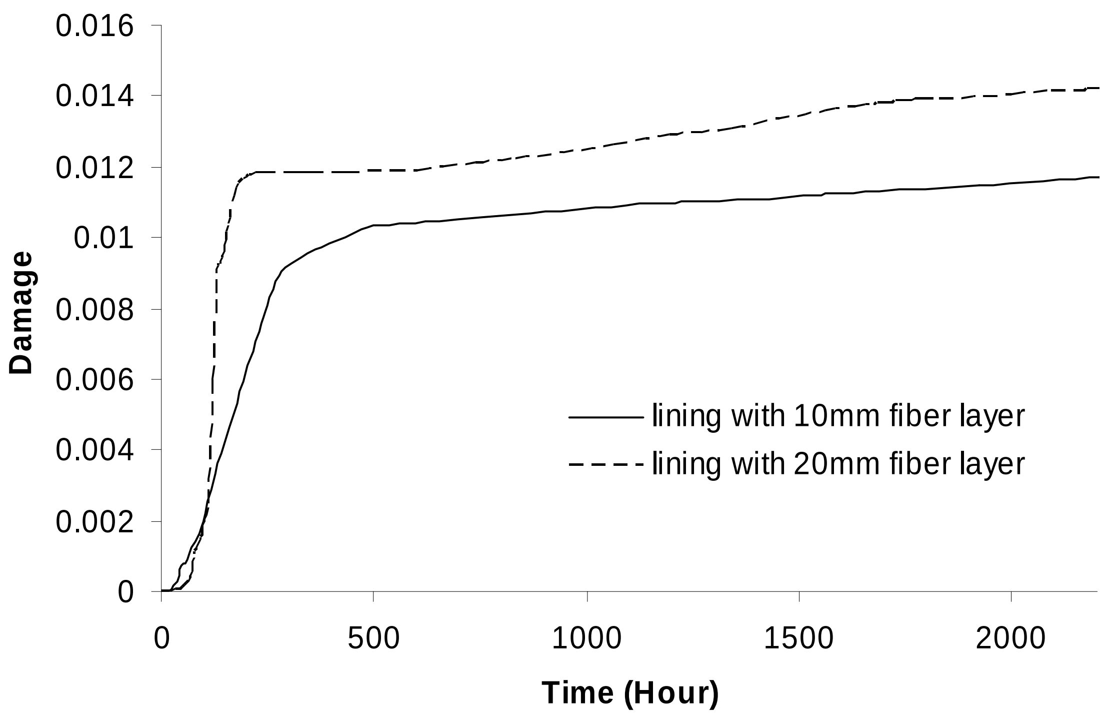

Figure 24 Tensile damage history in the refractory structure for two fiber layer thicknesses

CONCLUSION

Samples provided by in-kind sponsors were tested using cup testing. The best performing materials in the cup testing were fused cast materials. Currently testing of 2 castables were completed and 1 magnesia brick. Additional samples of magnesia castables have been provided. These appear to be outperforming any of the previously tested materials.

Computer simulation of existing materials will accelerate materials research in developing these new materials, and it is less costly and time consuming. Finite element modeling was conducted for the damage analysis in this study.

This study presented continuum damage mechanics based analytical model for predicting the failure behavior of refractory lining in high temperature black liquor gasifiers. The damage model accounts for the chemical expansion in addition to mechanical and thermal expansion. A comparison of predicted damage patterns for BLG refractory material with the observed damage pattern in a glass melting furnace refractory brick indicates that this model could be used to evaluate failure behavior of refractory linings in black liquor gasifier.

Chemical reaction causes the most compressive damage in the refractory structure. Layered damage occurred in the refractory structure due to the tensile damage. Expansion allowance affects the damage of the refractory structure. Tensile damage could be reduced by allowing for larger expansion. Compressive damage is not dependent on the expansion allowance provided by the fiber layer.

No systematic experimental work has been done so far to characterize the failure behavior of refractory materials in black liquor gasifier. Experimental work is needed to validate the damage model presented here.

REFERENCES

Stigsson, L. (1998): Chemrec^{TM} Black Liquor Gasification. *International Chemical Recovery Conference*, pp. 663-674.
Brown, C. A.; Hunter, W. D. (1998): Operating Experience at North America's First Commercial Black Liquor Gasification Plant. *International Chemical Recovery Conference*, pp. 655-662.
Dickinson, J. A.; Verrill, C. L.; Kitto, J. B. (1998): Development and Evaluation of a Low-Temperature Gasification Process for Chemical Recovery from Kraft Black Liquor. *International Chemical Recovery Conference*, June 1-4.
Taber, W. A. (2003): Refectories for Gasification. *Refectories Applications and News*, Vol. 8[4], pp. 18-22.
Larson, E. D.; Consonni, S.; Katofsky, R. E. (2003): A Cost-Benefit Assessment of Biomass Gasification Power Generation in the Pulp and Paper Industry. *Final report, Princeton University, Navigant Consulting, Inc., and Dipartimento di Energetica.*
Brown, C.; Landalv, I. (2001): The Chemrec Black Liquor Recovery Technology – A Status Report. *International Chemical Recovery Conference*, Whistler, B.C.
Kelleher, E. G.; Kohl, A. L. (1986): Black Liquor Gasification Technology. *Presented at the 1986 Summer National Meeting*, American Institute of Chemical Engineers, August 24-28.
Peascoe, R. A.; Keiser, J. R.; Hubbard, C. R.; Brady, M. P.; Gorog, J. P. (2001): Performance of Selected Materials in Molten Alkali Salts. *International Symposium on Corrosion in the Pulp & Paper Industry*, pp. 189-200.
Brown, C. A.; Leary, R.; Gorog, J. P.; Abdullah, Z. (2004): The Chemrec Black Liquor Gasifier at New Bern – A Status Report. *2004 International Chemical Recovery Conference*, pp. 1089- 1093.
Kachanov, L. M. (1958): Rupture Time under Creep Conditions. *Izv. Acad. Nauk USSR, OTN*, Vol. 8, pp. 26-31.
Lemaitre, J. (1985): A Continuum Damage Mechanics Model for Ductile Fracture. *J. Engrg. Mat. and Technol.*, Vol. 107[1], pp. 83-89.
Kachanov, L. M. (1986): Introduction to Continuum Damage Mechanics. Martinus Nijhoff Publishers, Dordrecht, the Netherlands.
Chaboche, J. L. (1988): Continuum Damage Mechanics, Part I & II. *J. Appl. Mech.*, Vol. 55, pp. 59-72.
Hillerborg, A.; Modeer, M.; Petersson, P. E. (1976): Analysis of Crack Formation and Crack Growth in Concrete by Means of Fracture Mechanics and Finite Elements. *Cement and Concrete Research*, Vol. 6, pp. 773-782.
Lubliner, J.; Oliver, J.; Oller, S.; Oñate, E. (1989): A Plastic-Damage Model for Concrete. *International Journal of Solids and Structures*, Vol. 25, pp. 299-329.
Lee, J.; Fenves, G. L. (1998): Plastic-Damage Model for Cyclic Loading of Concrete Structures. *Journal of Engineering Mechanics*, Vol. 124[8], pp. 892-900.
Saetta, A.; Scotta, R.; Vitaliani, R. (1998): Mechanical Behavior of Concrete Under Physical-Chemical Attacks. *Journal of Engineering Mechanics*, pp. 1100-1109.
Schacht, C. A. (1995): Refractory Linings. Marcel Dekker, Inc.
Boisse, P.; Gasser, A.; Rousseau, J. (2002): Computations of Refractory Lining Structures Under Thermal Loadings. *Advances in Engineering Software*, Vol. 33, pp. 487-496.

Buyukozturk, O.; Tseng, T. (1982): Thermomechanical Behavior of Refractory Concrete Lining. *Journal of the American Ceramic Society*, Vol. 65[6], pp. 301-307.
Chen, E. (1990): Simulation of the Thermomechanical Behavior of Monolithic Refractory Lining in Coal Gasifier Environment. *Radex Rundschau*, Vol. 4, pp. 376-384.
Hibbitt, Karlsson & Sorensen, INC. (2002): ABAQUS/Standard User's Manual. Version 6.3.
Hemrick, J. G. (2001): Creep Behavior and Physical Characterization of Fusion-Cast Alumina Refractories. PhD Dissertation, University of Missouri-Rolla.
http://www.matweb.com. MatWeb.com, a division of Automation Creations, Inc.
http://www.ceramics.nist.gov. NIST WebSCD Database, Ceramic division, National Institute of Standards and Technology.

BIBLIOGRAPHY

"Coal Gasification for Power Generation", http://www.dti.gov.uk/energy/developep/chevron_texaco_part2.pdf

"Gasification of Solid and Liquid Fuels for Power Generation", Technology status report to Department of Trade and Industry, 1998, http://www.dti.gov.uk/energy/coal/cfft/cct/pub/tsr008.pdf

"ABAQUS/Standard User's Manual," version 6.3, Hibbitt, Karlsson and Sorensen, Inc., 2000

"Refractories Handbook," The Technical Association of Refractories, Japan, 1998

A. R. Cooper, Jr, W. D. Kingery, "Dissolution in Ceramic Systems: I, Molecular Diffusion, Natural Convection and Forced Studies of Sapphire Dissolution in Calcium Aluminum Silicate", J. Am. Ceram. Soc, 47 [1], 37- 43, 1964.

Alexander Klein, "Gasification: An Alternative Process for Energy Recovery and Disposal of Municipal Solid Wastes", Master Thesis, Columbia University, 2002,

Ayhan Demirbas, "Pyrolysis and Steam Gasification Processes of Black Liquor," Energy Conversion and Management, 43, 877-884, 2002

B. N. Samaddar, W. D. Kingery, A. R. Cooper, "Dissolution in Ceramic Systems: II, Dissolution of Alumina, Mullite, Anorthite, and Silica in a Calcium-Aluminum-Silicate Slag", J. Am. Ceram. Soc, 47 [5] 249-254.

Barrie H. Bieler, "Corrosion of AZS, Zircon and Silica Refractories by Vapors of NaOH and of Na_2CO_3", *J. Am. Ceram. Soc. Bull*, **61**[7], 745-749, (1982).

Brown, N.R. "Alkali Vapor Attack of Alumino-Silicate refractories", Proceedings of International Ceramic Conference: AUSTCERAM 88, Sydney, pp.711-715, (1988).

C. A. Brown and W. D. Hunter, "Operating Experience at North America's First Commercial Black Liquor Gasification Plant", International Chemical Recovery Conference, 655-662, 1998

C. Brown, I. Landalv, "The Chemrec Black Liquor Recovery Technology – A Status Report," 2001 International Chemical Recovery Conference, Whistler, B.C., 2001

C. Wagner, "The Dissolution Rate of Sodium Chloride with Diffusion and Natural Convection as Rate-Determining Factors", J. Phys. Colloid Chem., 53, 1030-33, 1949.

Craig A. Brown and W. Densmore Hunter, "Operating Experience at North America's First Commercial Black Liquor Gasification Plant", International Chemical Recovery Conference, 655-662, 1998

Craig A. Brown, Ray Leary, J. Peter Gorog and Zia Abdullah, "The Chemrec Black Liquor Gasifier at New Bern – A Status Report," 2004 International Chemical Recovery Conference, 1089- 1093, 2004

D. A. Weirauch Jr, J. E. Lazaroff and P. D. Ownby, "Wetting in an Electric Packaging Ceramic System: II, Wetting of Alumina by a Silicate Glass Melt under Controlled PO_2 conditions," J. Am. Ceram. Soc., **78** [11] 2923-28 (1995).

Dave G. Newport, Lee N. Rockvam and Robert S. Rowbottom, "Leading Paper-Black Liquor Steam Reformer Start-up at Norampac," Presented at 2004 International Chemical Recovery Conference, Charleston, SC, June, 2004

Dominic Au, S. Cockcroft and D. Maijer, "Crack Defect Formation During Manufacture of Fused Cast Alumina Refractories," Metallurgical and Materials Transactions, **33A**, 2053-2065, 2002

E. G. Kelleher and A. L. Kohl, "Black Liquor Gasification Technology", Presented at the 1986 Summer National Meeting, American Institute of Chemical Engineers, August 24-28, 1986

E. Gmelin, M. Asen-Palmer, M. Reuther and R. Villar, "Thermal Boundary Resistance of Mechanical Contacts between Solids at Sub-ambient Temperatures," J. Phys. D: Appl. Phys. **32** R19-R43, 1999

E. Marotta, S. Mazzuca and J. Norley, "Thermal Joint Conductance for Graphite Materials," http://www.electronics-cooling.com

EnSheng Chen, "Simulation of The Thermomechanical Behavior of Monolithic Refractory Lining in Coal Gasification Environment," Radex Rundschau, 4, 376-384, 1990

Eric D. Larson and Delmar R. Rqymond, "Commercializing Black Liquor and Biomass Gasifier/Gas Turbine Technology", TAPPI Journal, 50 – 57, 1997

Eric D. Larson, Stefano Consonni, and Ryan E. Katofsky, "A Cost-Benefit Assessment of Biomass Gasification Power Generation in the Pulp and Paper Industry," Final report, Princeton Unversity, Navigant Consulting, Inc., and Dipartimento di Energetica, 2003

Gupta Abha, Rajan Nidhi, Mathur R.M. and Kulkarni A.G., "Development of Lignin By-Products for Industrial Applications", IPPTA Convention, 13, 49-55, 2001

http://www.ceramics.nist.gov

http://www.matweb.com

J. A. Dickinson, C. L. Verrill and J. B. Kitto, "Development and Evaluation of a Low-Temperature Gasification Process for Chemical Recovery from Kraft Black Liquor," International Chemical Recovery Conference, June 1-4, 1998

J. E. Lazaroff and P. D. Ownby, "Wetting in an Electric Packaging Ceramic System: I, Wetting of Tungsten by Glass in Controlled Oxygen Partial Pressure Atmospheres," J. Am. Ceram. Soc., **78** [3] 539-44 (1995).

J. G. Hemrick, "Creep Behavior and Physical Characterization of Fusion-Cast Alumina Refractories", PhD Dissertation, University of Missouri-Rolla, 2001

J. Gullichsen, H. Paulapuro, "Chemical Pulping, Paper Making Science and Technology", Book 6B.

J. Rawers, J. Kwong, and J. Bennett, "Characterizing Coal-gasifier Slag-refractory Interactions," Materials at High Temperatures, 16[4] 219-222, 1999

J. Sweeney and M. Cross, "Analyzing the Stress Response of Commercial Refractory Structures in Service at High Temperatures, II. A Thermal Stress Model for Refractory Structures," Trans. J. Br. Ceram. Soc., 81, 47-52, 1982

James Cantrell, P.E., "Simulation of Kraft Black Liquor Gasification – A Comparative Look at Performance and Economics", Engineering/Fishing & Converting Conference & Trade Fair, 1181-1195, 2001

K. Andreev, H. Harmuth, “FEM Simulation of The Thermo-mechanical Behaviour and Failure of Refractories - A Case Study,” Journal of Materials Processing Technology, 143-144[1] 72-77, 2003

K. McAlister & E. Wolfe, “A Study of the Effects of Alkali Attack on Refractories Used in Incineration”, Proceedings of Incineration Conference, Albuquerque, New Mexico, pp.631-638 (1992).

Keijo Salmenoja, “Black-Liquor Gasification: Theoretical and Experimental Studies,”, Bioresource Technology, 46, 167-171, 1993

Ken Patrick, "Gasification Edges Closer to Commercial Readily with Three N.A. Mill Startups", PaperAge, 30-33, 2003

Kennedy, Christophere R, “Alkali attack on mullite refractory in the grand forks energy technology center slagging gasifier”, *Journal of Materials for Energy Systems*, **3**[N-1, June] 27-31, (1981).

Kenneth T. Hood and Gunnar B. Henningsen, "Black Liquor Gasification…Evaluation of Past Experience in order to Define the Roadmap of the Future Pathway", TAPPI Fall Conference & Trade Fair, 1451-1463, 2002

Kirk J. Finchem, "Black Liquor Gasification Research Yields Recovery Options for Future", 69[11] 51-59, 1995

L. Reed, L. R. Barrett, “The Slagging of Refractories, I. The Controlling Mechanism in Refractory Corrosion”, Trans. Brit. Ceram. Soc, 54, 671-676, 1955.

L. Reed, L. R. Barrett, “The Slagging of Refractories, II. The Kinetics of Corrosion”, Trans. Brit. Ceram. Soc. 63, 509-534, 1964.

Lars Stigsson, “ChemrecTM Black Liquor Gasification,” International Chemical Recovery Conference, 663-674, 1998

LeBlanc, John R, ”Brockway’s Lower Checker Sulfate Test”, *J. Can. Ceram. Society*, **52**, 58-60, (1983).

M. L. Millard, “The Effect of Microstructure on the Liquid Corrosion of Sodium Chloride and Aluminum Oxide”, Ph.D. Dissertation, Department of Ceramic Engineering, University of Missouri-Rolla, 1982.

M. M. Akiyoshi, R. Pereira, A. P. da Silva and V. C. Pandolfelli, “Thermal Conductivity of Refractories,” American Ceramic Society Bulletin, **82** [6] 29-33, 2003

M. M. Yovanovich, ‘New XContact and Gap Correlations for Conforming Rough Surface,” AIAA-81-1164, presented at AIAA 16th Thermophysics Conference, Palo Alto, CA., June 1981

M. P. Borom, R. H. Arendt, “Dissolution of Oxides of Y, Al, Mg, and La by Molten Fluorides”, Ceramic Bulletin, 60 [11], 1169-1174, 1981.

Magnus Marklund, "Black Liquor Recovery: How Does It Work?" ETC, (Energy Technology Center, Sweden, http://www.etcpitea.se/blg/document/PBLG_or_RB.pdf

Mikael Ahlroth, Gunnar Svedberg, “Case Study on Simultaneous Gasification of Black Liquor and Biomass in a Pulp Mill,” International Gas Turbine & Aeroengine Congress & Exhibition, 1998

N. McCallum, L. R. Barrett, “Some Aspects of the Corrosion of Refractories“, Trans. Brit. Ceram. Soc., 51, 523-543, 1952.

Oral Buyukozturk and Tsi-Ming Tseng, “Thermomechanical Behavior of Refractory Concrete Lining,” Journal of the American Ceramic Society, 65[6] 301-307,1982

P. D. Ownby, Ke Wen K. Li, D. A. Weirauch Jr, “High Temperature Wetting of Sapphire by Aluminum,” J. Am. Ceram. Soc., **74** [6] 1275-81 (1991).

R. A. McCauley, “Corrosion of Ceramics”, 1994, New York, Marcel Deker.

R. A. Peascoe, J. R. Keiser, “Performance of Selected Materials in Molten Alkali Salts”, 10th International Symposium on Corrosion in the Pulp and Paper Industry (10th ISCPPI); Marina Congress Center, Helsinki, Finland, pp189-200, 2001.

R. A. Peascoe, J. R. Keiser, C. R. Hubbard, J. P. Gorog, C. A. Brown and B. H. Nilsson, “Comparison of Refractory Performance in Black Liquor Gasifiers and A Smelt Test System,” 2001 International Chemical Recovery Conference, Whistler, B.C., 2001

R. A. Peascoe, J. R. Keiser, C. R. Hubbard, M. P. Brady and J. P. Gorog, “Performance of selected materials in molten alkali salts,” International Symposium on Corrosion in the Pulp & Paper Industry 2001, 189-200, 2001

R. B. Hetnarski, “Thermal Stresses I,” Elsevier Science Publications B.V., 1986

R. Sangiorgi, “Corrosion of Ceramics by Liquid Metals”, NATO ASI Ser., Ser E., Applied Sciences, Vol. 267, pp. 261-84, 1994

Robert A. Peascoe, James R. Keiser, Camden R. Hubbard, Michael P. Brady and J. Peter Gorog, “Performance of selected materials in molten alkali salts,” International Symposium on Corrosion in the Pulp & Paper Industry 2001, 189-200, 2001

S. E. Feldman, W. K. Lu, “Kinetics of the Reactions between Silica and Alumino-Silicate Refractories and Molten Iron”, Metallurgical Transactions, 5, 249-253, 1974.

S. L. Cockcroft, J. K. Brimacombe, D. G. Walrod and T. A. Myles, “Thermal Stress Analysis of Fused-Cast AZS Refractories during Production: Part II, Development of Thermo-elastic Stress Model,” J. Am. Ceram. Soc., **77** [6] 1512-1521, 1994

S. Song, M. M. Yovanovich and F. O. Goodman, “Thermal Gap Conductance of Conforming Surface in Contact,” Journal of Heat Transfer, **115**, 533-540, 1993

Shigekastu Mori et. al., "Gasification Process of Organic Wastes for Electric Power Generation by Fuel Cell", http://www.cape.canterbury.ac.nz/Apcche_Proceedings/APCChE/Data/720REV.pdf

Suat Yilmaz, “Thermomechanical Modeling for Refractory Lining of a Steel Ladle Lifted by Crane,” Steel Research, 74[8] 485-490, 2003

Tadaoki Fukui, “Corrosion of Zircon Refractories by Vapors of Sodium Compounds”, *Ashi Gavasu Kenkya Hokoku*, **17**(2), 77-98 (1967).

Terry N. Adams, “Black Liquor Properties, Crystallization, and Sodium Salt Scaling in Concentrators,” TAPPI 2001 Pulping Conference, 1209-1222, 2001

Thomas, Everett A, “A Study of Soda and Potash Vapor Attack on Super Structure Refractories”, *J. Can. Ceram. Soc*, **44**, 37-41 (1975).

V. G. Levich, “Physicochemical Hydrodyanamics”, 1962. Englewood Cliffs, NJ, USA, Prentice-Hall.

V. W. Antonetti and M. M. Yovanovich, “Thermal Contact Resistance in Microelectronic Equipment,” in “Thermal Management Concepts in Microelectronic Packaging from Component to System,” ISHM Technical Monograh Series 6984-003, 135-151, 1984

W. A. Taber, “Refractories for Gasification,” Refractories Applications and News, **8**[4] 18-22, 2003

W. D. Kingery, H. K. Bowen, D. R. Uhlmann, “Introduction to Ceramics”, Second ed. , John Wiley & Sons. New York, 1976.

W. E. Lee, S. Zhang, “Melt Corrosion of Oxide and Oxide-Carbon Refractories”, A Review from Dept. of Engineering Materials, University of Sheffield, UK., 1999.

Xiaoting Liang, “Modeling of Thermomechanical, Cracking and Creep Behavior in Glasstank Crown,” MS Thesis, University of Missouri-Rolla, 2003

Y. A. Cengel and R. H. Turner, “Fundamentals of Thermal-Fluid Sciences,” McGraw-Hill Higher Education, 2001

Y. Chung, “Corrosion of Partially Stabilized Zirconia by Steelmaking Slags”, M.S. Thesis, Department of Ceramic Engineering, University of Missouri-Rolla, 1993.

Y. Kuromitsu, H. Yoshida, “Interaction between Alumina and Binary Glasses”, J. Am. Ceram. Soc, 80 [6] 1583-87, 1997.

Yamaguchi, A, “Reactions between Alkaline Vapors and Refractories for Glass Tank Furnaces”, Proceedings of International Congress on Glass, Kyoto, Japan, pp.1-8 (1974).